JOURNAL OF MATERIALS SCIENCE 35 (2000) 4749–4762

# Dry sliding wear behavior of spray deposited AlCuMn alloy and AlCuMn/$SiC_p$ composite

MANCHANG GUI
*Beijing Institute of Aeronautical Materials, Beijing, 100095, People's Republic of China*
SUK BONG KANG, JUNG MOO LEE
*Korea Institute of Machinery and Materials, Changwon, 641-010, Korea*
*E-mail: sbkang@kmail.kimm.ye.kr*

The dry sliding wear behavior of spray-deposited Al-Cu-Mn alloy and its composite reinforced with 13 vol.% SiC particles have been studied in the applied load of 5–400 N (corresponding normal stress is 0.1–8 MPa). It showed that SiC particle-reinforced AlCuMn composite produced by spray deposition process exhibited an improved wear resistance at the entire applied load range in comparison to the monolithic alloy. However, this improvement was not significant in the overall load range. With increasing the applied load, the wear rate of the composite and the monolithic alloy exhibited four different regions, therefore the wear was dominated by different wear mechanism. The former three regions all belonged to mild wear. The transition from mild to severe wear occurred at the similar critical load for both the composite and the monolithic alloy. For both the composite and the monolithic alloy, with increasing applied load, the dominant wear mechanism exhibited successively: oxidative mechanism, delamination mechanism, subsurface-cracking-assisted adhesive mechanism and adhesive mechanism. 

## 1. Introduction

Particle-reinforced aluminum matrix composites show a superior combination of mechanical and physical properties, such as high modulus and strength, high-temperature stability, excellent wear resistance and heat conductivity, low coefficient of thermal expansion and density in comparison to monolithic aluminum alloys [1–3]. The composites have been considered as potential application in the tribological field, and are becoming a favorite material as piston, rotor brake, bearing sleeve, cylinder liner and compressor scroll [4–6]. The tribological behavior of particle-reinforced aluminum matrix composites has been extensively studied during the last 20 years [7–15]. Various particle reinforcements including SiC, $Al_2O_3$, $Si_3N_4$, $TiB_2$, $B_4C$ and graphite have been involved in these studies. The tribological behaviors, i.e. wear rate and wear mechanism of the composites in dry sliding wear are influenced by two kinds of factor; (1) experimental conditions including load, sliding speed, atmosphere, temperature and counterpart material, (2) reinforcement characteristics including volume fraction and size of particle reinforcement, distribution of the reinforcement in aluminum matrix and bonding of the reinforcement/matrix interface. Up till now, detailed reports on the effect of load in a wide range on the dry sliding wear behavior of particle-reinforced aluminum matrix composites are limited. Alpas and Zhang [7] experimentally reported that three wear regimes existed with increasing load for the composites of 6061 alloy reinforced with $Al_2O_3$ particles and 2124 alloy reinforced with SiC particles. At low loads, the particles support the applied load, and the wear resistance of the composites is at least an order of magnitude better than that of monolithic aluminum alloys. When the particles are fractured due to the increase in the applied load, the wear rate of the composites are comparable to those of the monolithic alloys. The reinforcements delay the transition from mild to severe wear. Zhang *et al*. [16] reported that two wear regions existed with increasing applied load for SiC and $Al_2O_3$ particle-reinforced aluminum composites. The transition between two regions is the critical load from mild to severe wear. In general, aluminum matrix composites reinforced with SiC or $Al_2O_3$ particles have been found to improve the wear resistance under dry [12, 17, 18] and lubricated sliding wear [19]. However, Saka and Karalekas [20] observed a decrease in the sliding wear resistance with increasing $Al_2O_3$ particle volume fraction. Alpas and Embury [21] showed that SiC reinforcement does not contribute to the wear resistance of aluminum alloys under the conditions where SiC particles promote subsurface cracking and removal by delamination. The improved wear resistance of particle-reinforced aluminum matrix composites is related to mechanical mixed layer (MML) formed in worn subsurface [22]. Venkatarman *et al*. [15] have done a detailed investigation on the worn subsurface, and shown a correlation between the thickness of MML and wear rate.

Spray deposition process is one of main routes to produce particle-reinforced aluminum matrix composites. The process has the advantage that the contact time between melt and reinforcement is short, so reaction between the two is limited, and the grain size of the resulting composite is relatively uniform and fine. In addition, the presence of the particles during solidification of spraying droplet also refines the matrix microstructure. The composites produced by spray deposition process possess potential superior mechanical properties. However, the report about the wear resistance behavior of the composites produced by this process has hardly been found.

The aims of present work are, in a wide range of applied load, to study the dry sliding wear behavior of a spray-deposited Al-Cu-Mn alloy and its composite reinforced with 13 vol.% SiC particles, and to achieve a full understanding on the wear mechanism of the materials.

## 2. Experimental procedures

AlCuMn alloy and its composite reinforced with 13 vol.% SiC particles were produced by spray deposition process. The compositions of the AlCuMn alloy are listed in Table I. The average size of the SiC particles is about 10 $\mu$m. Wear testing was carried out in the TE92 type unidirectional pin-on-disc machine (Plint and Partners Ltd.). Wear test specimens in the form of $\Phi 8 \times 15$ mm cylindrical block were machined from forged rods with a deformation ratio of 13 : 1. The counterpart material was cold work hardened AISI D2 tool steel disc. The hardness of the discs was $730 \pm 10$ VHN. Two pins were used during each test. The applied load was varied from 5–400 N (corresponding normal stress is 0.1–8 MPa). Sliding speed and distance were kept constant at 0.8 m/s and 1.5 km, respectively. However, in the case of severe wear, i.e. at 375 and 400 N, due to strong noise and vibration, the wear test was ended at a sliding distance of 500 m. To perform the test under T6 condition, the age curves of two materials were established. The Vickers microhardness was measured under a load of 200 g and averaged from eight readings using a Matsuzawa MXT70 microhardness tester. The results are shown in Fig. 1. Two materials were solutionized at 530 °C for 30 min in a salt bath, quenched in cold water and artificially aged at 190 °C for different time in an oil bath. The aging peaks of the monolithic alloy and the composite exhibited at 5 h and 4 h, respectively.

The test specimens were ground on 800 grit emery paper to have uniform initial surface. The weight loss during wear test was measured using an electronic balance with the resolution of $\pm 0.01$ mg. The specimens were thoroughly cleaned with acetone in ultrasonic cleaner before and after the wear test. Wear rate was calculated by dividing weight loss by sliding distance.

TABLE I Compositions of the AlCuMn alloy

| Element | Cu | Mn | Mg | Ti | Zr | V | Al |
|---|---|---|---|---|---|---|---|
| Wt% | 6.35 | 1.82 | 0.42 | 0.46 | 0.28 | 0.22 | Bal. |

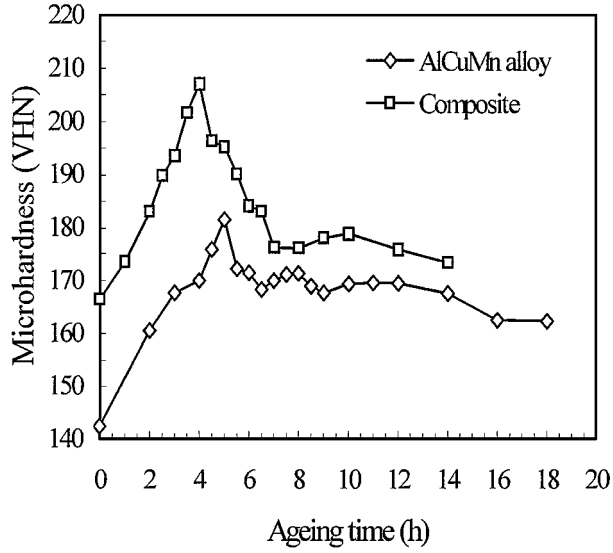


*Figure 1* Age hardness behavior of the AlCuMn alloy and its $SiC_p$-reinforced composite at 190 °C.

Worn surface and subsurface were characterized by using JEOL 8600 type scanning electron microscope (SEM) attached with energy dispersive X-ray analyses (EDX), optical microscope and micro-hardness tester. The worn specimens were sectioned parallel to the sliding direction and perpendicular to the sliding surface using low speed diamond wheel to observe the subsurface of the worn specimens. The cut specimens were cold mounted and polished, and then done optical microscopic observation. Rigaku X-ray diffractometer (XRD) was used to analyze the phase constituent of the tested materials and wear debris using Cu $K_\alpha$ radiation under condition of 40 kv and 30 mA.

## 3. Results

### 3.1. Microstructure

Fig. 2 shows the typical microstructure of the AlCuMn alloy and AlCuMn/$SiC_p$ composite at T6 condition. X-ray diffraction analysis (Fig. 3) indicated that main second phases, $Al_2Cu$ and $MnAl_6$ are contained in the $\alpha$Al matrix. In Fig. 2a, a very uniform distribution of small $Al_2Cu$ and $MnAl_6$ particles with about 2 $\mu$m in mean size can be seen in the Al matrix. In the case of the composite, a good bonding between $SiC_p$ and aluminum matrix was achieved (Fig. 2b). The SiC particles exhibit a random distribution in the Al matrix. The microhardness of the AlCuMn alloy and AlCuMn/$SiC_p$ composite in the test condition is 180 and 210 VHN, respectively.

### 3.2. Wear

#### *3.2.1. Effect of applied load on the wear rates*

Fig. 4 shows the effect of applied load on the wear rates of the monolithic alloy and the composite in the load range of 5–400 N. In the entire applied load range, the composite improves wear resistance in comparison to the monolithic alloy. However, the improvement is not the same magnitude as that observed in other composites [23, 24]. In general, the wear rates decrease by

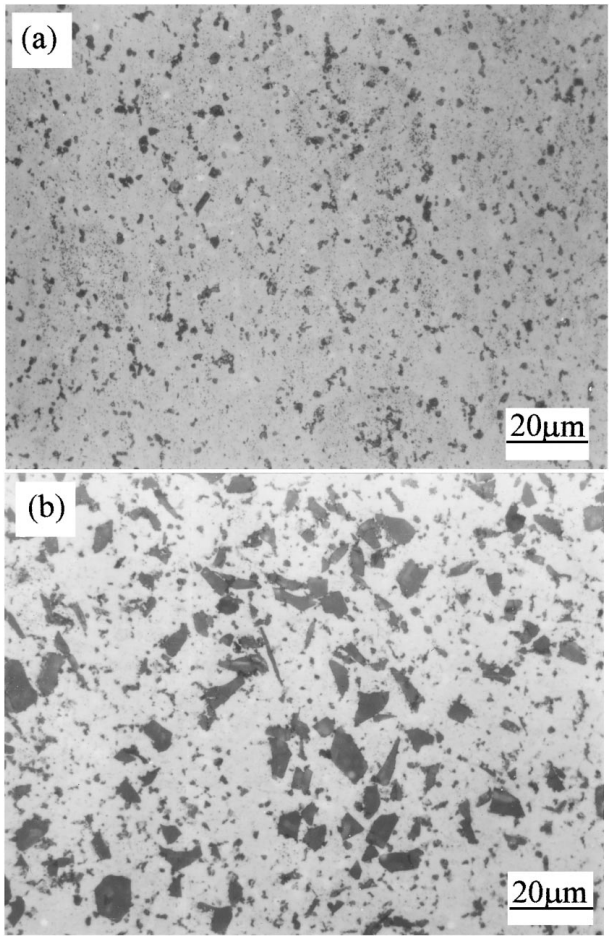


*Figure 2* Typical microstructure of the AlCuMn alloy and AlCuMn/$SiC_p$ composite at T6 condition, (a) AlMnCu alloy and (b) AlCuMn/$SiC_p$ composite.

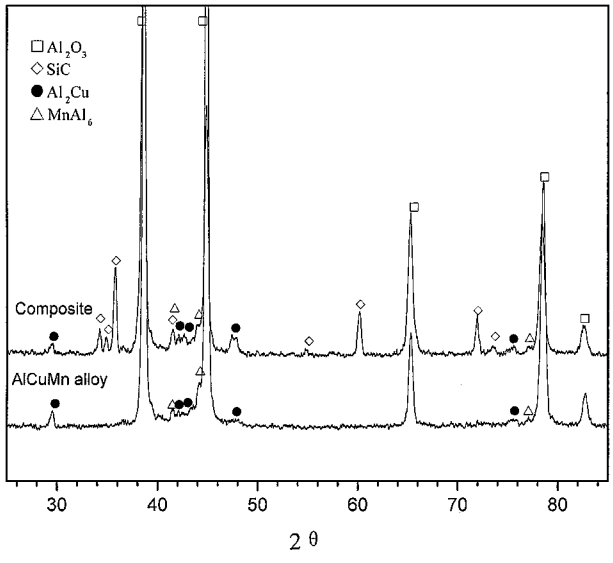


*Figure 3* X-ray diffraction patterns for the AlCuMn alloy and AlCuMn/$SiC_p$ composite.

10–50%, whereas only at low loads of less than 10 N, more than 100% decrease in the wear rate is obtained. The tendency of the wear rate variation with the applied load is consistent for two materials. In Fig. 4, the wear rate curves reveal that there exists four different regions, which are marked as region I, II, III and IV from low to high load. In region I, the applied load is

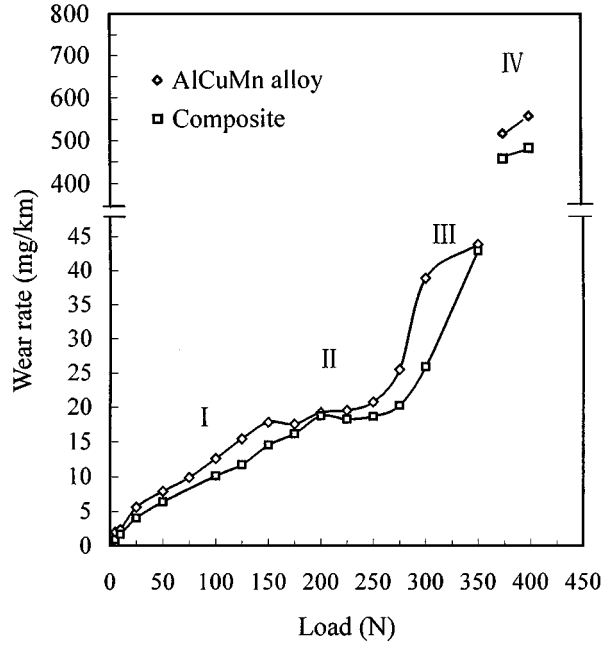


*Figure 4* Effect of applied load on wear rates in the load range of 5–400 N.

located below 200 N and 150 N, respectively, for the composite and the monolithic alloy. Near linear functions of wear rate to the applied load are demonstrated. The wear rate increases with increasing load at a ratio of about 0.09–0.11 mg/km·N for two materials. The region II is located in the load range of 150–250 N for the monolithic alloy, and 200–275 N for the composite. In this region, a considerably slow change (almost a plateau) of the wear rate with increasing load is displayed. When the applied load surpasses 250 N for the monolithic alloy and 275 N for the composite, the wear rates of two materials increase rapidly with increasing load (region III). A transition in the wear rate between region III and IV is present, and the transition load is the same for both the composite and the monolithic alloy. Evidently, the transition stands for the one from mild to severe wear, as has been reported in other literatures [7, 16]. The wear rate increases about one order of magnitude at the transition load for two materials. The four regions exhibit distinct wear characteristics, i.e. different wear mechanisms. It will be discussed in the later content.

### 3.2.2. Worn surface

The worn surfaces of the composite pins at different applied loads are shown in Fig. 5. At low load of 25 N, the worn surface appears smooth and consisted with small grooves (Fig. 5a). In addition, few small dimples (about 100 $\mu$m in length) are also seen in the surface. The worn surface is grey visually. However, with increasing load, it gradually becomes bright, and a full metallic gloss appears after the applied load is beyond 125 N. Generally, from region I to III, the width of groove and the size of dimple on the worn surface increase with increasing load. Fig. 5b and c correspond to the load of 200 N. The worn surface is also smooth, and the width of groove is larger than that at the load of 25 N. In addition, larger dimples are easily found

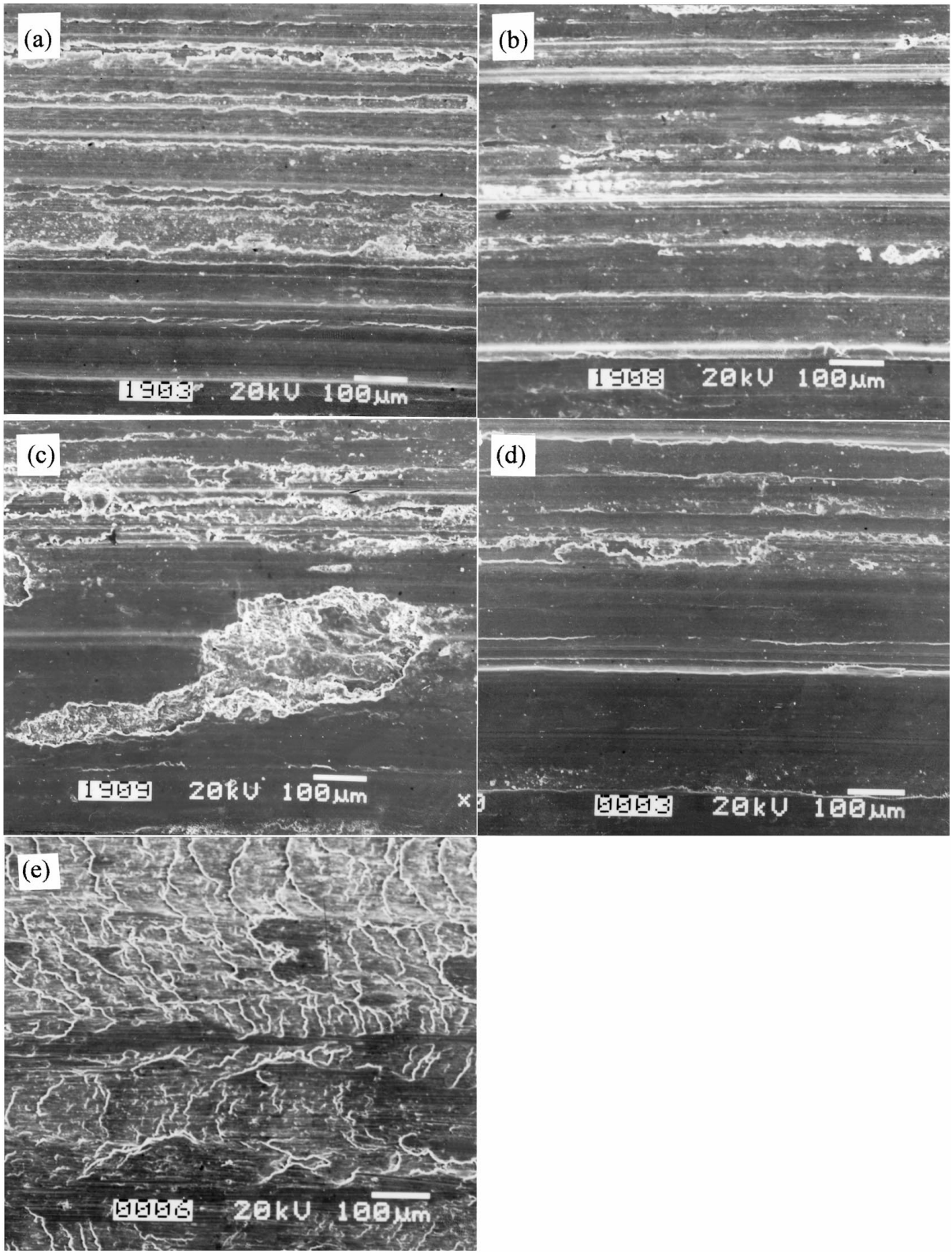


*Figure 5* Worn surfaces of the composite pins at different applied load; (a) 25 N, (b) 200 N, (c) 200 N, showing the dimples, (d) 350 N and (e) 400 N.

(Fig. 5c). Fig. 5d, which corresponds to the load of 350 N, shows large and smooth grooves at the worn surface. In fact, the entire worn surface consists of smooth groove area and large rough patch region. Fig. 5e represents the worn surface at the load of 400 N, and shows a series of stripes like river wave. In this case, a great amount of material transfer from the pin to the disc occurred, and the wearing track in the disc was covered by the material of pin. The rubbing surface of the pin no longer directly contacted with the disc.

The worn surfaces of the monolithic alloy at different applied loads are shown in Fig. 6. In the entire applied load range, the characteristics of worn surface of pin are similar to those exhibited in the composite. However, the width of groove in the worn surface increases more rapidly with increasing load. Fig. 6d, which corresponds to the load of 350 N, shows large patches and irregular plastic flow lines indicating the occurrence of an extensive plastic deformation during wear. However, material transfer hardly occurred from the tested pin to

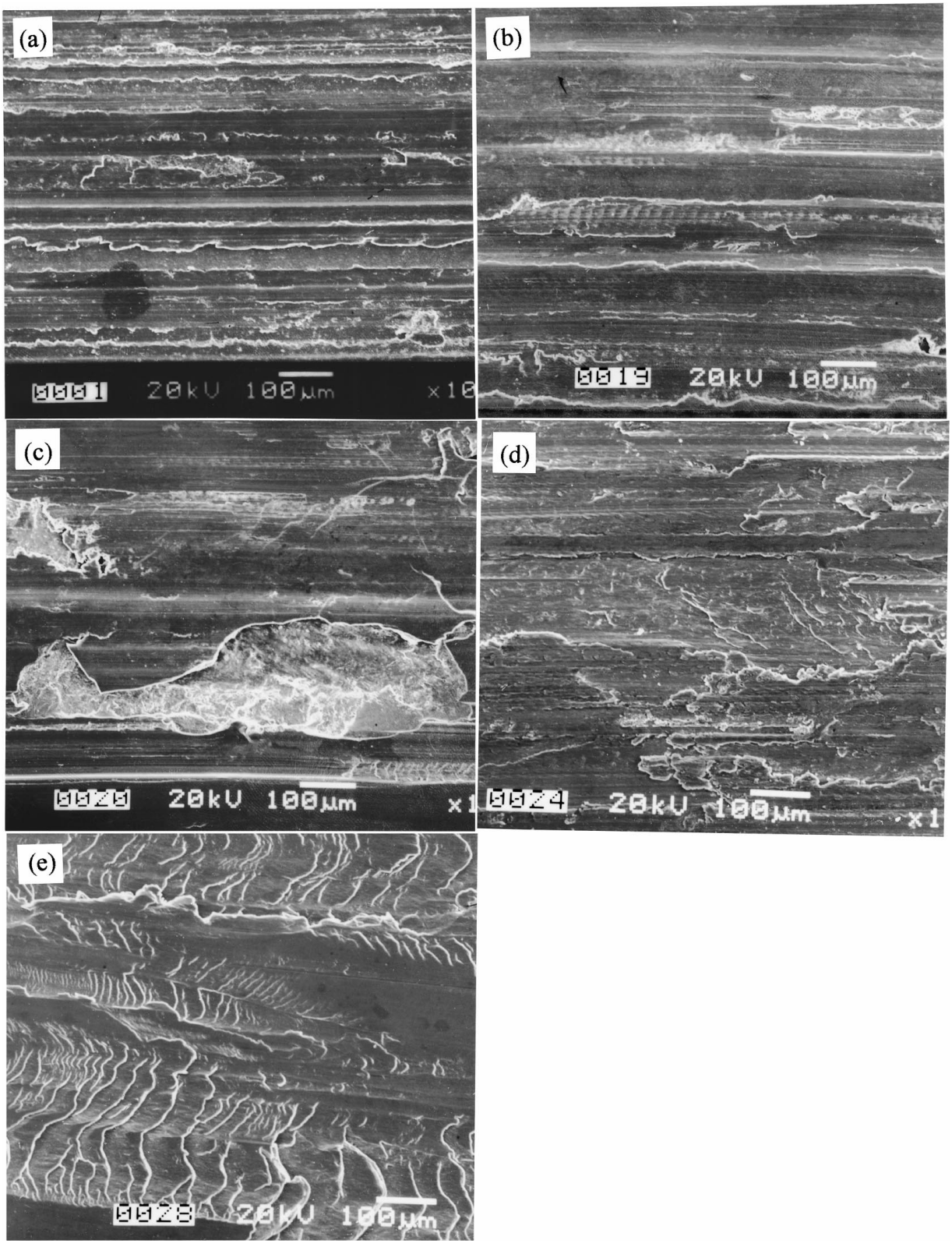


*Figure 6* Worn surfaces of the monolithic alloy pins at different applied load; (a) 25 N, (b) 200 N, (c) 200 N, showing the dimples, (d) 350 N and (e) 400 N.

the surface of disc, and wearing track in the disc remained clean. In general, an extensive plastic deformation at the worn surface is often observed in region III.

### 3.2.3. Subsurface

Figs 7 and 8 show the optical microstructures of the worn subsurface of the composite and the monolithic alloy at the applied loads of 25 N, 200 N, 350 N and 400 N, respectively (Arrows mark indicate the sliding direction). The microstructure clearly reveals a MML and bending of flow lines along the sliding direction for two materials. Systematic observation showed that the MML exhibits discontinuity in worn specimens besides the case of no MML. The thickness of the MML increases with increasing of applied load, and reaches a maximum in the end of region II, and then decreases and eliminates finally. In region III, the MML can be

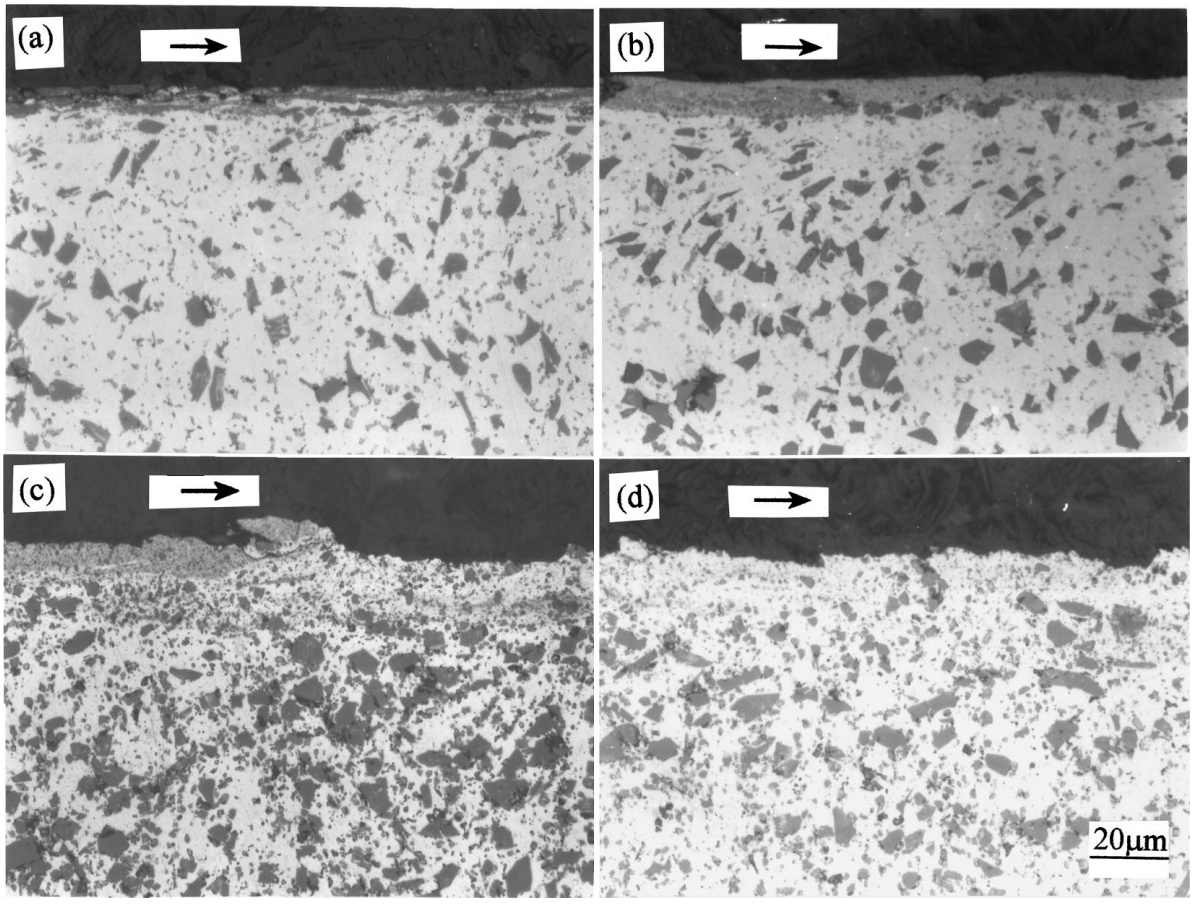


*Figure 7* Optical microstructures of the worn subsurface of the composite pins at different applied loads; (a) 25 N, (b) 200 N, (c) 350 N and (d) 400 N.

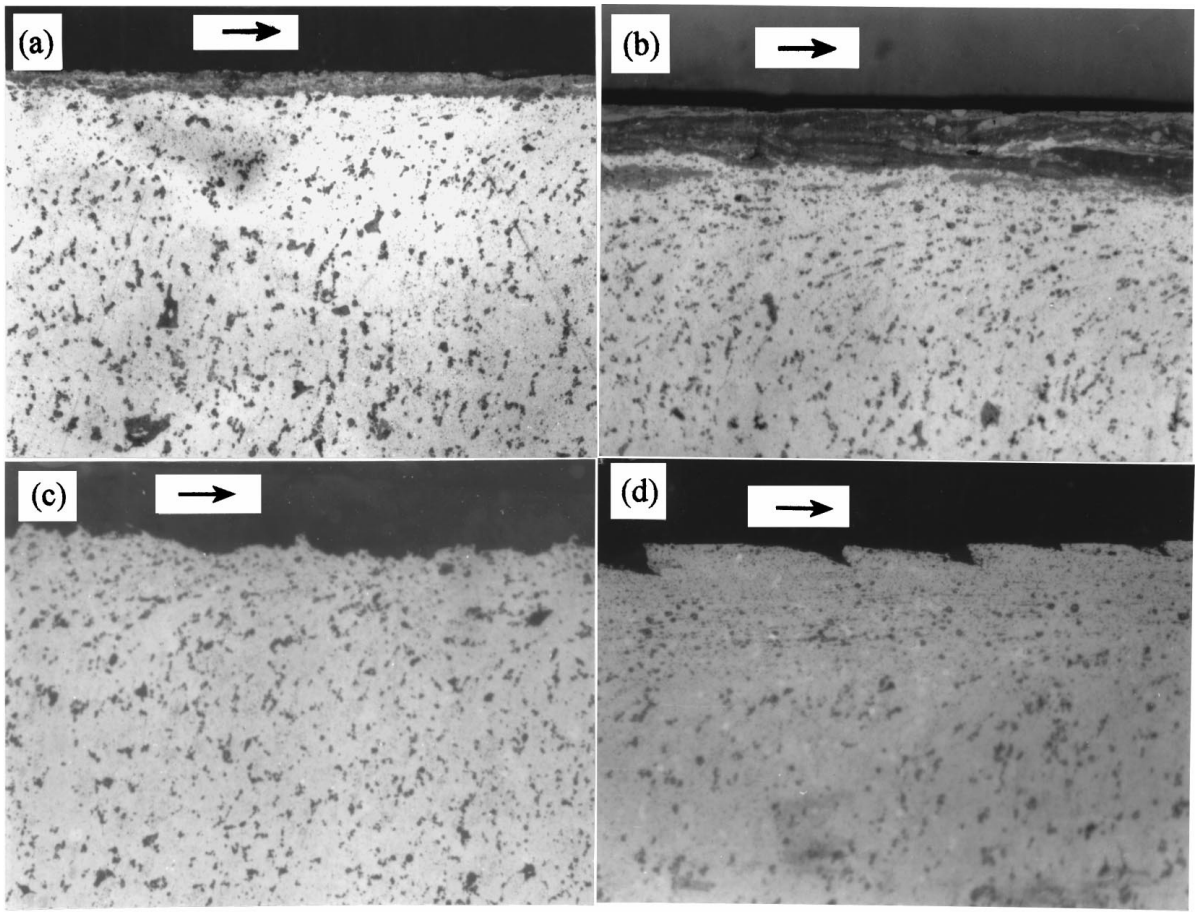


*Figure 8* Optical microstructures of the worn subsurface of the monolithic alloy pins at different applied loads; (a) 25 N, (b) 200 N, (c) 350 N and (d) 400 N.

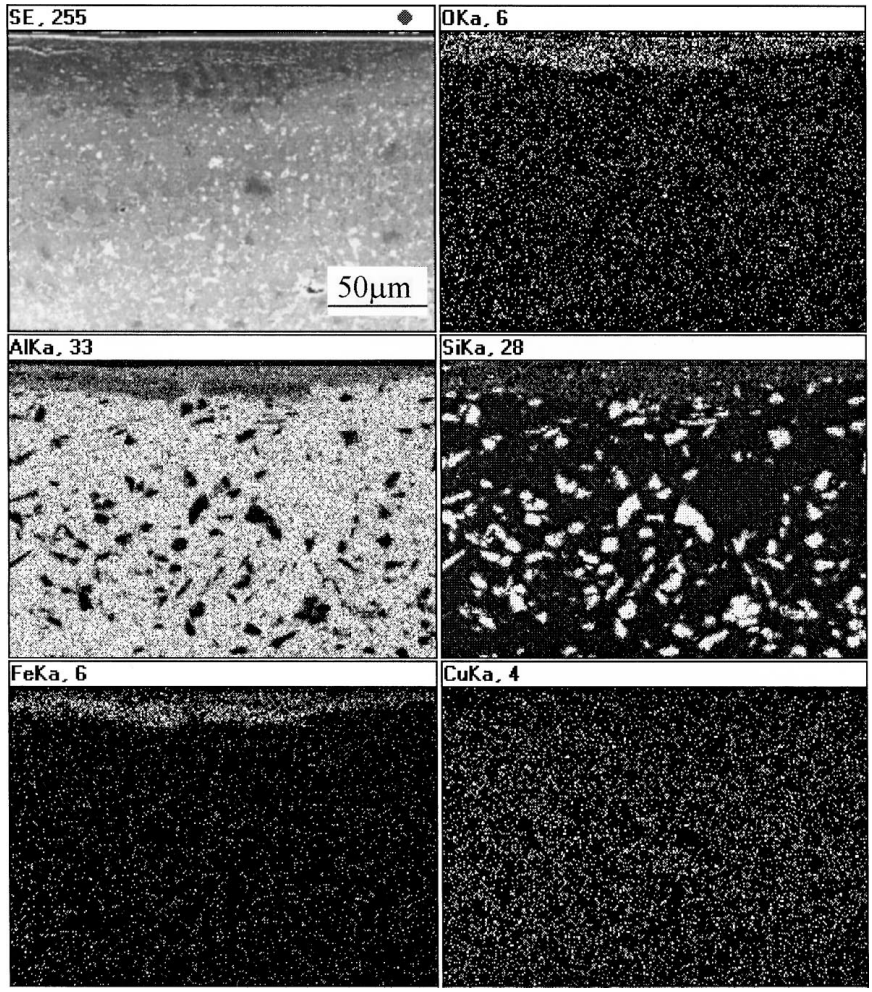


*Figure 9* SEM micrograph and the corresponding Al, O, Fe, Si, and Cu dot-map images showing MML at the subsurface of worn pins of the composite.

found only in the small part of the worn subsurface for the composite at the load of 350 N, and no MML can be observed in the monolithic alloy at the loads of 300 and 350 N. In addition, some large dimples and cracks in the subsurface can be also seen. In the case of 400 N, as shown in Figs 7d and 8d, a distinct subsurface appears, and some prows are observed, which indicates a typical adhesive wear [25]. The size of the prow in the monolithic alloy is much larger than that in the composite, and the shape is more regular. The reason is mainly that the monolithic alloy has a better ductility, and hence allows a larger plastic deformation, which results in larger wear debris. Figs 9 and 10 show SEM micrographs and the corresponding Al, O, Fe, Si and Cu dot-map images on the worn subsurface at the load of 200 N for the composite and the monolithic alloy, respectively. The average compositions from five points at the MMLs by EDX quantitative analyses for the composite and the monolithic alloy are listed in Table II. It is found that the MML is a featureless mixture of iron and oxygen-rich phase for both the composite and the monolithic alloy. On the other hand, the composition of the MML displays some difference at different spots in the same specimen. The microhardness of the MML at some applied loads was measured using 25 g load. The hardness values of the MML are listed in Table III. It is found that the hardness of MML is substantially higher than the bulk hardness, and the hardness value hardly changes with increasing load. In addition, the hardness of MML in the composite is higher than that in the monolithic alloy.

TABLE II EDX quantitative analyses at the MML at the load of 200 N

| | Level (wt. %) | | | | | | |
|---|---|---|---|---|---|---|---|
| Materials | O | Al | Si | Cr | Mn | Fe | Cu |
| Monolithic alloy | 13.79 | 62.10 | - | 2.35 | 1.03 | 15.87 | 4.57 |
| Composite | 24.27 | 42.02 | 7.94 | 2.60 | 0.96 | 19.39 | 2.80 |

TABLE III Microhardness (VHN) of MML of pin generated at different loads

| | Load (N) | | | |
|---|---|---|---|---|
| Materials | 25 | 125 | 200 | 250 |
| Monolithic alloy | 455 | 442 | 448 | 463 |
| Composite | 748 | 772 | 760 | 754 |

### 3.2.4. Wear debris

The observation and analysis of the wear debris are a key factor to understand the wear mechanism. In the present work, the wear debris generated at different load was collected. SEM observation and XRD analysis indicated that the morphology of wear debris and its

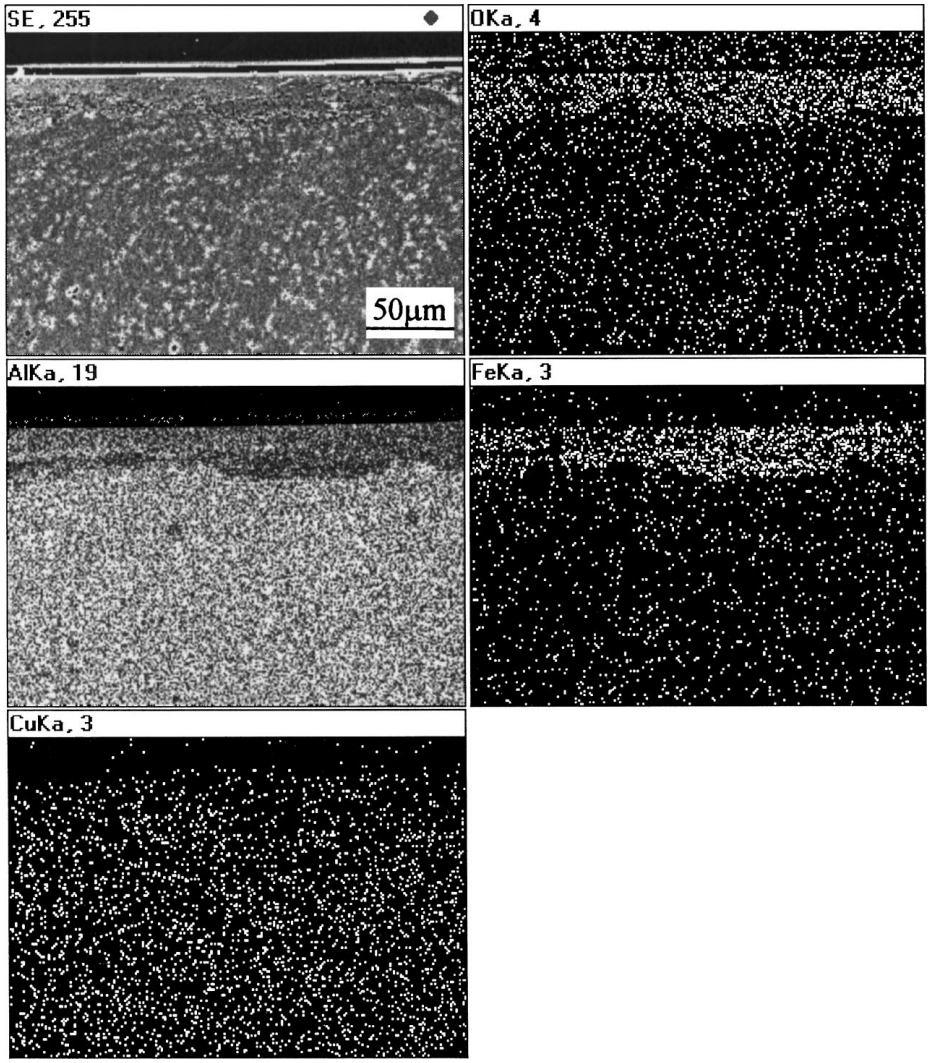


*Figure 10* SEM micrograph and the corresponding Al, O, Fe and Cu dot-map images showing MML at the subsurface of the worn pins of the monolithic alloy.

constituent change with the applied load. XRD patterns of the wear debris of the composite and the monolithic alloy at different loads are shown in Figs 11 and 12, respectively. In the case of 400 N, the constituent of the

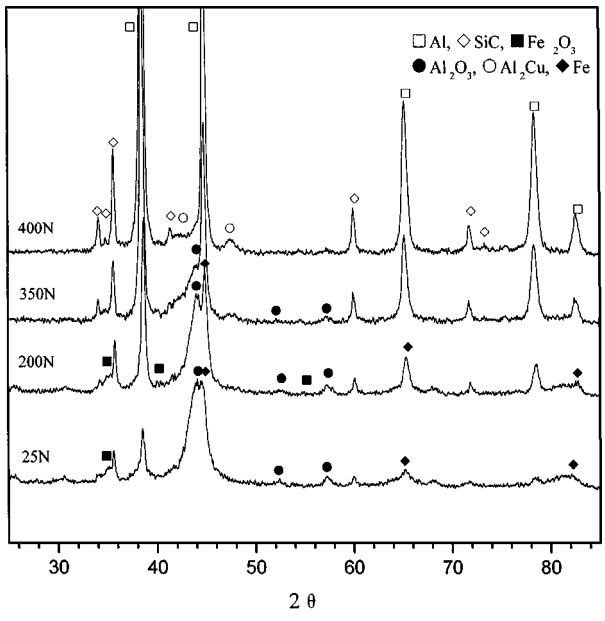


*Figure 11* XRD diffraction patterns of the wear debris of the composite at different loads.

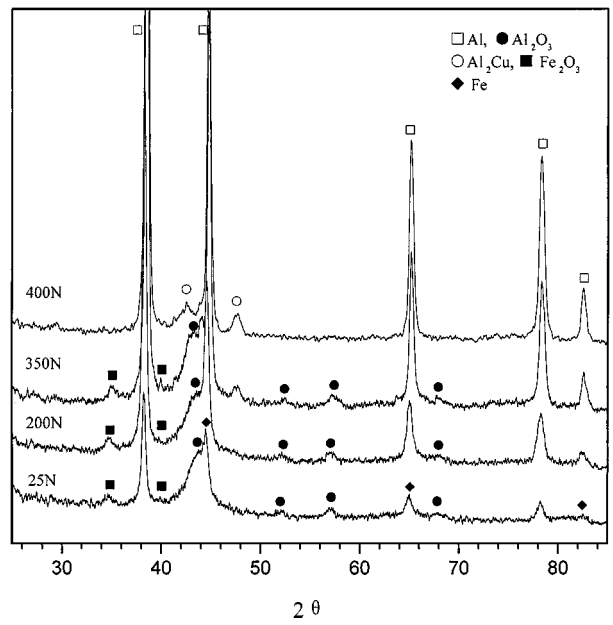


*Figure 12* XRD diffraction patterns of the wear debris of the monolithic alloy at different loads.

wear debris shows the same composition as that of bulk pin material for both the composite and the monolithic alloy. When the applied load is below 350 N, the wear debris contains $Al_2O_3$ and $Fe_2O_3$. Especially, at low

TABLE IV Results of EDX quantitative analysis of debris generated at different load

| Material | Load (N) | Level (wt. %) Al | Fe | O | Si | Cu |
|---|---|---|---|---|---|---|
| Monolithic alloy | 25 | 58.69 | 20.83 | 10.85 | - | 5.43 |
| | 200 | 75.94 | 9.58 | 7.21 | - | 4.55 |
| | 350 | 82.58 | 3.54 | 5.48 | - | 6.28 |
| | 400 | 89.95 | - | - | - | 6.44 |
| Composite | 25 | 44.66 | 32.54 | 5.73 | 6.74 | 4.63 |
| | 200 | 44.88 | 33.09 | 4.51 | 6.69 | 4.50 |
| | 350 | 62.83 | 13.82 | 3.92 | 10.90 | 4.99 |
| | 400 | 76.46 | - | - | 13.50 | 6.45 |

loads such as 25 and 50 N, strong peaks of $Al_2O_3$ and $Fe_2O_3$ can be seen. In the patterns, three main peaks of Fe overlap those of Al. However, according to the experimental result obtained by other investigators [7, 13], pure Fe should be present in the debris of wear system composed of composite (or aluminum alloy) and steel. Table IV shows the results of EDX quantitative analysis about the level of main elements in the debris generated at different load. It is found that the debris generated at 400 N shows the same composition as that of bulk material, and high levels of Fe and O are contained in the debris at the load of 25 and 200 N. Relative small amount of Fe and O exist in the debris at the load of 350 N. In addition, the Fe levels in the composite debris are higher than those in the monolithic alloy debris, indicating that the SiC particles have stronger abrasive wear to the steel disc.

SEM was used to observe the morphology of wear debris. Figs 13 and 14 show the scanning electron micrographs of wear debris of the composite and the monolithic alloy at different loads, respectively. In region I, especially under 100 N, the wear debris is mainly powder-like and dark in color visually. At the load of 25 N, the size of wear debris is less than 10 $\mu$m. After the load of 100 N, shiny metallic pieces debris appear in the wear debris and its amount increases with increasing load for two materials. In region II, the wear debris is composed of fine powders and irregular shaped platelets or flakes. The small and dark powders in the wear debris remain up to the load of 350 N. At the load of 400 N, the wear debris is in form of irregular shaped platelets.

## 4. Discussion

### 4.1. Wear rate

The present wear tests indicated that the AlCuMn/$SiC_p$ composite produced by spray deposition process exhibits an improved wear resistance at the entire

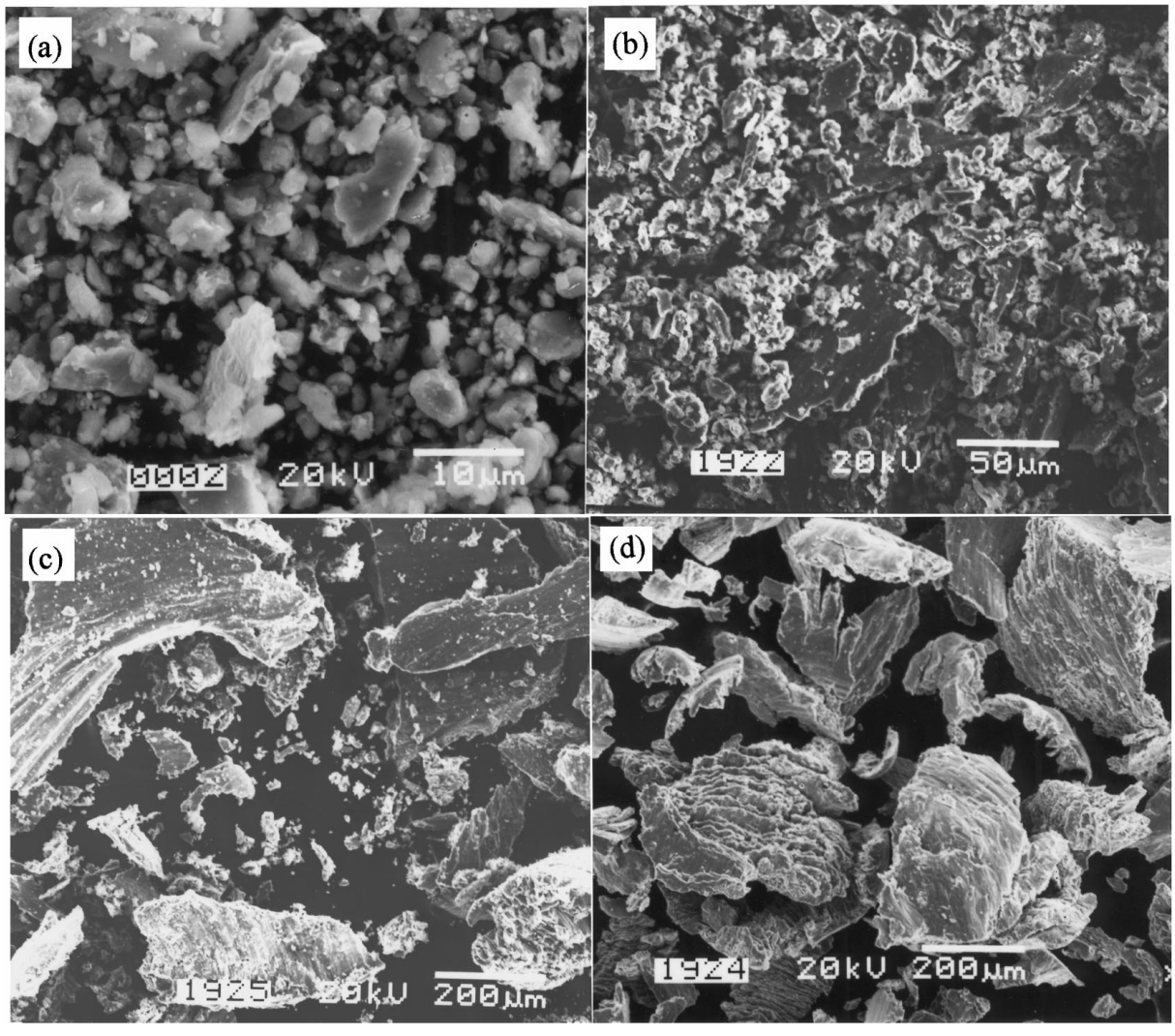


*Figure 13* Scanning electron micrographs of wear debris of the composite at different loads; (a) 25 N, (b) 200 N, (c) 350 N and (d) 400 N.

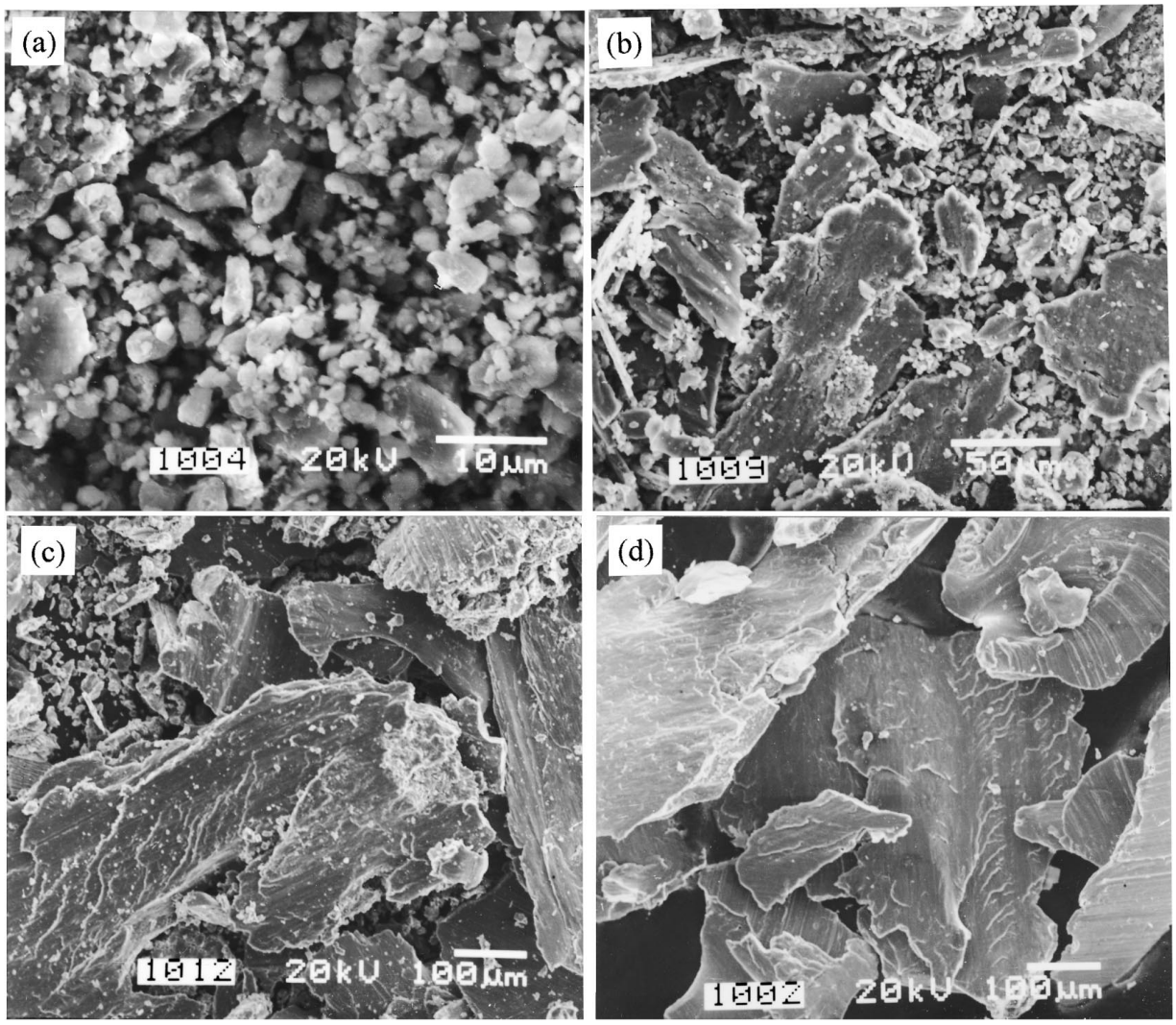


*Figure 14* Scanning electron micrographs of wear debris of the monolithic alloy at different loads; (a) 25 N, (b) 200 N, (c) 350 N and (d) 400 N.

applied load range of 5–400 N (corresponding normal stress is 0.1–8 MPa) in comparison to the monolithic alloy. However, this improvement is not significant in the overall applied load range. For example, at 25, 225, 300, 350 and 400 N, the wear rates of the composite record 4.0, 18.2, 25.8, 42.8 and 478 mg/km respectively, and at the same loads, the wear rates of the monolithic alloy record 5.6, 19.5, 38.5, 43.8 and 553 mg/km. The decrease in the wear rate is not more than 50% at these loads. For cast Al-Si alloy or wrought aluminum alloy such as 6061 and 2024 Al, the differences in the wear rate between these alloys and their $SiC_p$-reinforced composites have been reported in a lot of literatures [7, 9, 13, 23, 24]. In general, a great improvement in wear resistance has been revealed by SiC particle reinforcement although there were also contrary results. Manish Roy *et al*. [9] observed a decrease by a factor of 3-4 in the wear rate by 10–20 vol.% $SiC_p$. In addition, the influence of $SiC_p$ reinforcement on the wear rate also depends on experimental factors, mainly including sliding velocity and applied load. Wang *et al*. [13] reported that wear rates of 7091 Al and 7091/20$SiC_p$ composite are of the same order of magnitude when the sliding velocity is less than 1.2 m/s, and a significant decrease occurs when the sliding velocity is greater than 1.2 m/s. In the present work, the composite and the monolithic alloy have the same order of magnitude in the wear rate although the SiC reinforcement improved the wear resistance to a certain extent. The main reason is that the monolithic alloy has a fine $\alpha$Al grain and uniform distribution of fine second phase particles due to rapid solidification, and the second phase particles, $Al_2Cu$ and $MnAl_6$ which have a higher hardness, can be also considered as a kind of reinforcement. Therefore, the monolithic alloy itself exhibits a good wear resistance. In addition, it has been found that the wear rate of SiC particle-reinforced aluminum composites is considerably influenced by volume fraction of the reinforcement, and higher volume fraction of SiC particles led to greater improvement in wear resistance [9, 12, 23, 24]. So the limited amount of $SiC_p$ reinforcement in the composite is another possible reason for that.

### 4.2. Wear regime and mechanical mixed layer

For the relation of wear rate and applied load, i.e. wear regime, Alpas and Zhang [7] reported that three wear regimes existed with increasing load for SiC particle-reinforced composites. At low loads of below 10 N

(regime I), the particles support the applied load, and the wear resistance of the composites is at least an order of magnitude better than that of monolithic aluminum alloys. In the intermediate load range (regime II), the wear rate of the composite is comparable to that of monolithic alloys and increases gradually with increasing load. A second transition occurs at the end of regime II, and then severe wear becomes dominant (regime III). However, Pramila Bai *et al*. [12] indicated experimentally that there was no transition of wear rate at range of the 2–26 MPa pressure in A356/$SiC_p$ and steel wear system. Zhang *et al*. [16] showed that two regions of wear existed with increasing applied load for SiC and $Al_2O_3$ particle-reinforced aluminum composites. The transition between two regions is the critical load from mild to severe wear. As a common rule, for Al-Si alloys or their particle-reinforced composites, a severe wear regime would be encountered when the applied load reaches a critical value and the wear rate in severe regime is about one order of magnitude greater than that in the former region [16, 26]. In the present work, the four regions exist apparently with the variations of the wear rate and the applied load. It should be noted that no discontinuity appears between the regions in the former three regions. The variation of wear rate from region I to III is not significant. Meanwhile, the wear features, such as worn surface and wear debris display gradual change from one region to another one. Therefore, these three regions all belong to mild wear. One transition occurs at a load of between region III and IV. As has been reported earlier [16, 26], the wear rate increases more than one order of magnitude at the transition load in the present two materials. Clearly, the transition is the one from mild to severe wear, thus severe wear is presented in region IV. In addition, SiC reinforcement displays no influence on the transition load.

Mechanical mixed layer (MML) plays an important role in the wear of SiC particle-reinforced aluminum composites [15, 26] and cast Al-Si alloy [27]. Venkataraman *et al*. performed hardness measurement of MML. It showed that the MML formed on the worn surfaces of $SiC_p$-reinforced aluminum composite is substantially harder than the bulk material (the hardness of MML is 6–8 times higher than that of corresponding matrix material) because it contains a fine mixture of Fe, Al and SiC phases. They also pointed out that the width of the MML increased with increasing load. However, Alpas and Zhang [7, 26] reported that the MML exists only under the low load condition of less than 10 N (about 0.2 MPa). The absence of MML at worn subsurface of matrix alloy was considered as the reason that the wear resistance of aluminum matrix alloy is worse than that of composite [15, 26]. In the present work, at 5–275 N for the monolithic alloy and 5–350 N for the composite, MML can be always observed. While, at higher loads (in region III), MML displays very unstable. The MML is found to contain Fe and O. The source of Fe in the MML is obviously originated from the steel disc counterpart. It is very likely that the hard particles (including SiC and $Al_2Cu$) at the worn surface plough into the counterface and thus create debris containing mainly iron. The debris from the steel counterface, together with the debris from pin, compacted to form the MML on the worn surface. The Fe in the MML was in two forms of pure $\alpha$-Fe and $Fe_2O_3$. The hardness of the MML is substantially higher than that of the bulk material due to the presence of Fe and Al oxides. The higher hardness in the MML of the composite than that in the monolithic alloy is attributed to the existence of SiC and oxides. Clearly, in the present materials, the MML is a protective layer, and improves the wear resistance of the materials. The improved wear resistance in the composite can be explained based on the fact that there exist higher hardness values in MML and bulk material by comparison to the monolithic alloy.

### 4.3. Wear mechanism

The wear tests showed that the wear rate exhibited different characteristics in the different regions. Therefore, the wear should be controlled by different wear mechanism. In region I, for both the composite and the monolithic alloy, XRD analysis (Figs 11 and 12) showed that the wear debris produced in this region contain a great amount of oxides of Al and Fe. Furthermore, the wear debris is very fine powder and dark in color, indicating that oxidative wear is the main wear mechanism. In addition, delamination of MML also plays an assisted effect, especially in late period of this region. The dimples in the worn surface provide the evidence for delamination. EDX analyses also indicate that the dimple zone has the identical composition with the MML. Fig. 15 is an EDX pattern of a dimple zone of the monolithic alloy at 25 N showing a high Fe and O levels, which proves that the dimple was formed from the removal of MML. Oxide formation, in particular $Fe_2O_3$ can act as solid lubricants [28, 29]. Thus, in this region, the wear rate increases slowly with increasing load.

In region II, the size of the dimple already becomes larger (The size at 200 N is about three times larger than

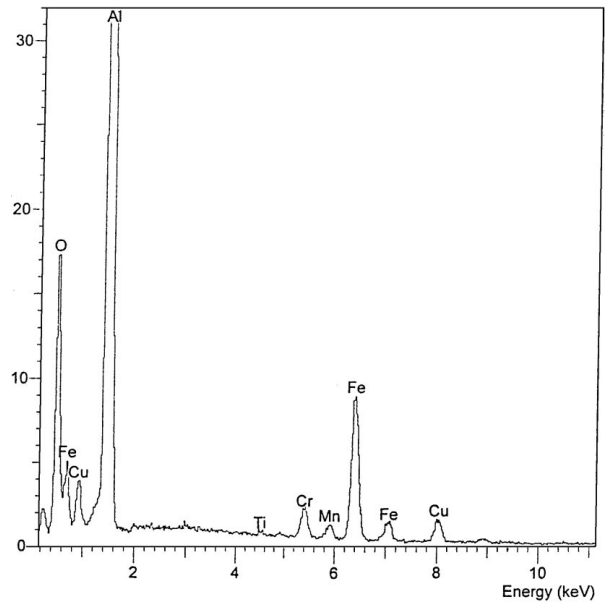


*Figure 15* EDX spectrum of a dimple zone of the monolithic alloy at 25 N showing a high Fe and O levels.

that at 25 N). The wear debris contains a lot of shiny metallic flakes together with some small and dark powder. The delamination takes place not only at MML but also at other subsurface zone. This can be proved by the larger flaky wear debris and subsurface observation. Some dimples are formed from the removal of the deformation layer of pin material beneath the worn surface by the way of crack initiation at SiC/Al interface and propagation. It is well known that delamination is a process of the initiation and propagation of subsurface crack. In the present wear test, few cracks can be observed on the worn surface, indicating that the crack initiation and growth which are required in delamination wear take place mainly in the subsurface. The wear rate in this region increases very slowly with the applied load, almost displays a plateau. This phenomenon was also observed in the SiC particle-reinforced A356 composite [26]. The reason is that the propagation of subsurface crack needs to meet a certain stress condition, and the crack can keep relative stability in a certain load range, resulting in a relative stable wear rate. Thus, in this region, delamination is the major wear mechanism, and oxidative wear is the assisted wear mechanism.

In region III, in the case of the monolithic alloy, an extensive plastic deformation of the pin material can be seen on the worn surface, and a certain amount of large irregular platelets can be observed in the wear debris. The shear fracture trace (river flow stripes) is clearly displayed in the surface of the large platelet, indicating the occurrence of adhesive wear during the wear process. In this region, the depth of the deformed layers below the worn surface becomes larger than that in region II, thus the crack is formed in the subsurface more easily, which in turn makes it difficult for any stable MML to form in the subsurface. In addition, because of thermal softening, the initiation of crack may also take place from the worn surface, as shown in Fig. 16a. The formation of large debris in this region is a process of crack initiation and propagation, which results in limited large wear rate. Therefore, the wear process is controlled mainly by subsurface-cracking assisted adhesive mechanism. For the composite, SiC particle can reduce the propensity of the plastic deformation of material at the rubbing surface, therefore increases the transition load from region II to III. At the load of 350 N, some worn surface exhibits severe plastic deformation although MML can be seen at some subsurface. The crack is easily seen in the subsurface of composite pin in region III (Fig. 16b). Therefore, its wear mechanism is consistent with that of the monolithic alloy. It should be noted that, in the former three regions, wear characteristics change smoothly between regions. Thus, the dominant wear mechanism can not be determined exactly in the transition zones between these regions.

In region IV, the shape of prow is formed in the subsurface, and XRD analysis (Figs 11 and 12) indicates that the wear debris has the same constituent as that of bulk pin material for both the composite and the monolithic alloy. A clean shear fracture (Figs 5e and 6e) can be seen on the worn surface. In addition, the steel disc was covered by the pin materials. These evidences show the occurrence of adhesive wear. The removal of material on the worn surface of pin occurs by shear fracture, and the process of the shear fracture is relatively quick, resulting in a high wear rate. Evidently, adhesive wear is the dominant wear mechanism in this region.

### 4.4. Transition from mild to severe wear

The transition from mild to severe wear can occur by different ways, such as the increase in applied load, sliding velocity as well as sliding distance. Kragelskii [30] proposed that the transition from mild to severe wear in ferrous material would occur when the temperature at the contact surface exceeded a critical temperature. Bowden and Tabor [31] suggested that a strong adhesion between two contact surfaces occurs at temperature of 0.4-0.5 melting point of the alloy. Zhang and Alpas [32] reported that the critical transition temperature in 6061 Al-SAE 52100 steel system corresponds to 0.42 of the melting temperature of the 6061 Al. At this temperature, thermally activated deformation processes are expected to become active and lead to the softening of the material adjacent to the contact surface. However, in the present work, when the applied load is beyond the critical value, severe wear occurred just at the beginning of wear test. In this condition, the temperature increase in the contact surface should be limited, therefore it is impossible to induce the significant softening

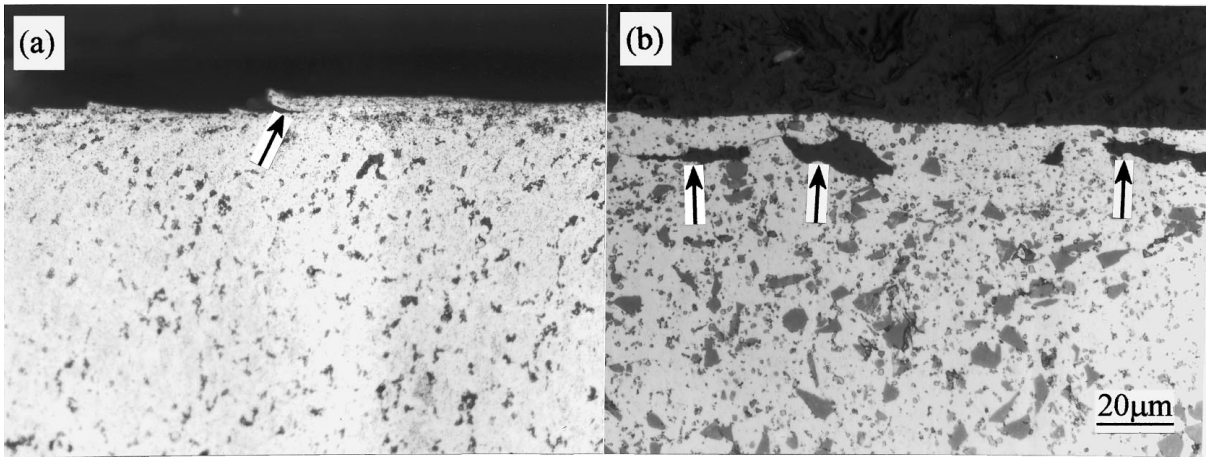


*Figure 16* Cracks in the subsurface of the monolithic alloy and the composite at the load of 350 N (arrows show the cracks); (a) monolithic alloy and (b) composite.

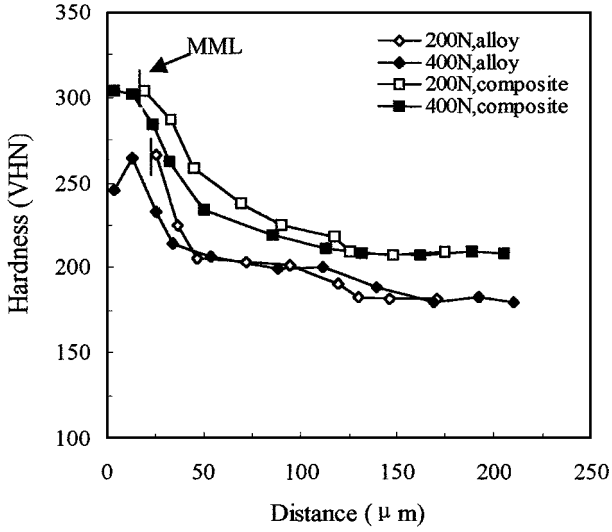


*Figure 17* Microhardness-depth profiles beneath the worn surfaces at the loads of 200 and 400 N for the monolithic alloy and the composite.

on the worn surface. Fig. 17 shows the microhardness-depth profiles beneath the worn surfaces at the loads of 200 and 400 N (the hardness was measured using a load of 10 g). It is seen that the hardness curves beneath the worn surface at the load of 400 N are similar to those beneath the MML at the load of 200 N. Only little softening at the worn surface is found for the monolithic alloy. It shows that no significant thermal softening of the material adjacent to the contact surface occurred for the two materials at the load of 400 N. Therefore, as for the load-induced transition in the present materials, the temperature at the contact surface is not a main factor to determine the transition to severe wear. Based on the mechanism in the severe wear mentioned above subsection, the shear fracture is attributed to the removal of material from the worn surface of pin. As the strain-induced shear stress created by applied load is larger than the shear strength of the material itself, the severe wear will occur. Therefore, the occurrence of severe wear depends on the strength of the material of pin and the strain-induced shear stress.

In some investigations [7, 9], it has been found that SiC or $Al_2O_3$ reinforcement increases the transition load, which can be explained that the reinforcement can improve the thermal stability of aluminum alloy. However, in this work, the SiC reinforcement doesn't show an influence on the transition load. Table V lists the typical mechanical properties of the monolithic alloy and the composite. It is clear that the SiC reinforcement mainly leads to an increase in the elastic modulus, and the monolithic alloy still maintains the excellent strength values. As has discussed above, the shear fracture, which depends on the strength of pin material, is the main mechanism in the severe wear region. However, in the present composite, the SiC reinforcement only gives a small increase in tensile strength, therefore negligible influence on the transition load.

TABLE V Typical mechanical properties of the monolithic alloy and composite

| | Room temperature | | | 200 °C | | |
|---|---|---|---|---|---|---|
| Materials | $\sigma_b$ (MPa) | $\sigma_{0.2}$ (MPa) | E (GPa) | $\sigma_b$ (MPa) | $\sigma_{0.2}$ (MPa) | E (GPa) |
| AlCuMn | 560 | 490 | 78 | 400 | 350 | - |
| AlCuMn/SiC | 561 | 509 | 92.5 | 407 | 370 | - |

## 5. Conclusions

In a wide range of applied load of 5–400 N, the dry sliding wear behaviors of spray-deposited Al-Cu-Mn alloy and its composite reinforced with 13 vol.% SiC particles have been studied. The following major conclusions can be drawn from the present investigation:

1. SiC particle-reinforced AlCuMn composite produced by spray deposition process exhibits an improved wear resistance at the entire applied load range of 5–400 N (corresponding normal stress is 0.1–8 MPa) compared to the monolithic alloy. This improvement is not significant in the overall applied load range. The wear rate of the composite and the monolithic alloy with increasing load can be divided into four regions. The former three regions all belong to mild wear. A transition from mild to severe wear occurs at the same critical load for both the composite and the monolithic alloy.

2. In region I, the wear debris is very fine powder and dark in color and contains oxides. The wear is controlled by oxidative mechanism, and delamination of MML also plays an assisted effect, especially in late period of the region.

3. In region II, delamination is the major wear mechanism, and oxidative wear is an assistant wear mechanism. The propagation of subsurface crack needs to meet a certain stress condition, and the crack can keep relative stability in a certain load ranges, resulting in a relative stable wear rate.

4. In region III, the wear is controlled mainly by subsurface-cracking-assisted adhesive mechanism. SiC particle can reduce the propensity of the plastic deformation of material at the rubbing surface, therefore increase the transition load from region II to III.

5. In region IV, adhesive wear is the dominant wear mechanism. Wear debris is formed by the shear fracture occurred in the subsurface. The severe wear depends on the strength of the material of pin and the strain-induced shear stress. SiC particles have no influence on the transition load.

## References

1. S. DERMARKAR, *Metall. Mater. Trans.* **2** (1986) 144.
2. D. E. HAMMOND, *Modern Casting* **8** (1989) 29.
3. D. J. LLOYD, *International Mater. Reviews* **39** (1994) 1.
4. J. E. ALLISON and G. S. COLE, *J. Met.* **45** (1993) 19.
5. D. O. KENNEDY, *Adv. Mater. Proc.* **6** (1991) 42.
6. S. X. HUANG and K. PAXTON, *JOM* **50**(8) (1998) 26.
7. A. T. ALPAS and J. ZHANG, *Metall. Mater. Trans.* **25A** (1994) 969.
8. R. A. SARAVANAN, J. M. LEE and S. B. KANG, *ibid.* **30A** (1999) 2523.
9. M. ROY, B. VENKATARAMAN, V. V. BHANUPRASAD, Y. R. MAHAJAN and G. SUNDARARAJAN, *Metall. Trans.* **23A** (1992) 2833.

10. A. T. ALPAS and J. ZHANG, *Script Metall. Mater*. **26** (1992) 505.
11. M. A. MARTINEZ, A. MARTIN and J. LLORCA, *ibid*. **28** (1992) 207.
12. B. N. PRAMILA BAI, B. S. RAMASESH and M. K. SURAPPA, *Wear* **157** (1992) 295.
13. A. WANG and H. J. RACK, *Mater. Sci. Eng*. **147A** (1991) 211.
14. A. RAVIKIRAN and M. K. SURAPPA, *Script Materialia* **36** (1997) 95.
15. B. VENKATARAMAN and G. SUNDARARAJAN, *Acta Mater*. **44** (1996) 461.
16. Z. F. ZHANG, L. C. ZHANG and Y. W. MAI, *J. Mater. Sci*. **30** (1995) 1961.
17. A SATO and R. MEHRABIAN, *Metall. Trans*. **7B** (1976) 443.
18. F. M. HOSKING, F. FOLARPORTILLO, R. WUNDERLIN and R. MEHRABIAN, *J. Mater. Sci*. **17** (1982) 477.
19. C. A. CARACOSTAS, W. A. CHIOU, M. E. FINE and H. S. CHENG, *Script Metall. Mater*. **27** (1992) 167.
20. N. SAKA and D. P. KARALEKAS, "Wear of Materials" (ASME, New York, 1991) p. 159.
21. A. T. ALPAS and J. D. EMBURY, "Wear of Materials" (ASME, New York, 1991) p. 784.
22. R. L. DEUIS, C. SUBRAMANIAN and J. M. YELLUP, *Comp. Sci. Technol*. **57** (1997) 415.
23. H. L. LEE, W. H. LU and S. L. CHAN, *Wear* **159** (1992) 223.
24. B. VENKATARAMAN and G. SUNDARARAJAN, *Acta Mater*. **44** (1996) 451.
25. O. VINCSBO and S. HOGMARK, "Fundamentals of Friction and Wear of Materials" (ASM, 1981) p. 373.
26. A. T. ALPAS and J. ZHANG, *Wear* **155** (1992) 83.
27. B. N. PRAMILA BAI and S. K. BISWAS, *Acta Metall*. **39** (1991) 833.
28. K. C. LUDEMA, *Wear* **100** (1984) 315.
29. S. C. LIM and M. F. ASHBY, *Acta Metall*. **35** (1987) 1.
30. I. V. KRAGELSKII, "Friction and Wear" (Butterworth and Co., London, 1965) p. 88.
31. F. P. BOWDEN and D. TABOR, "The Friction and Lubrication of Solids, Part II" (Oxford University Press, London, 1964) p. 97.
32. J. ZHANG and A. T. ALPAS, *Acta Mater*. **45** (1997) 513.

*Received 21 December 1999*
*and accepted 23 February 2000*